# DEVELOPMENT OF A SUPERCAPACITOR-BASED REGENERATIVE BRAKING TEST BED

Ping XU[1]

*Aiming at the problem that the real vehicle regenerative braking system cannot fully demonstrate the energy recovery process, a supercapacitor-based regenerative braking test bed is developed. The test bed is composed of three core modules: a kinetic energy simulation module for simulating vehicle inertia, an energy conversion and storage module for converting flywheel mechanical energy into electrical energy and storing it, and a control module for real-time monitoring and power transmission control. Then experimental tests were conducted to explore the influences of key parameters on braking distance and regenerative energy efficiency. Experiment results show that Initial speed is positively correlated with braking distance and regenerative efficiency, as higher speeds enhance the generator's electromagnetic induction. A lower transmission ratio shortens braking distance by 61.9%–64.7% and improves efficiency by up to 3.22%, due to increased generator rotational speed and stronger electromagnetic braking torque. A higher supercapacitor initial voltage extends braking distance but boosts efficiency to 53.2%, avoiding excessive Joule losses and nonlinear generator operation at low voltages. This test bed realizes low-cost, controllable simulation of regenerative braking which is useful to understanding of regenerative braking systems.*

**Key words:** Braking energy recovery; simulation; test bench; design and development

## 1. Introduction

Braking energy recovery technology, also called Regenerative Braking Systems (RBS) can effectively improve the energy efficiency of vehicles, especially for the Electric Vehicle (EV). Relevant studies show that the application of braking energy recovery technology can extend the cruising range of EVs by 10%-30% [1-3]. Therefore, braking energy recovery systems are widely used in different type vehicles. Such as, hybrid vehicle and EVs of Toyota, Honda, BYD and other automakers, are all equipped with braking energy recovery systems [4].

RBS can be divided into series, parallel and hybrid types [5-7]. And it also can be divided based on the energy storage component, such as batteries [8], hydraulic [9], flywheels [10], capacitors [11], pneumatic [12], etc. The essence of RBS is to convert kinetic energy into other forms of energy that are easy to store.

Supercapacitors, as an emerging energy storage technology, demonstrate remarkable advantages in multiple aspects, such as high in power density, fast in

[1] Lecture, Collage of Civil Engineering, Henan University of Engineering, Zhengzhou, China, e-mail: pingxu@haue.edu.cn

charging and discharging, long in cycle life, wide in usage temperature range, and safe in operation. Meanwhile, the energy conversion efficiency is over 90%. Compared with other ways of energy storage, supercapacitors show broad application prospects in the RBS. Researches done by the University of Michigan team showed that the RBS with supercapacitors can increase the braking energy recovery efficiency by 20%-30% in hybrid vehicles. Ouyang Minggao's team proposed a "supercapacitor-battery collaborative braking energy recovery strategy", which optimized the distribution of motor braking force and mechanical braking force through a fuzzy control algorithm, increasing the braking energy recovery efficiency of a pure electric vehicle to 58% under urban working conditions and shortening the braking distance by 7%. Prezi's study verified that the RBS using supercapacitors can recover more than 53% of braking energy in EVs and quickly release it to meet instantaneous power demand. Zou Zhongyue verified the efficiency of the RBS with supercapacitors and proved that the maximum regenerative braking energy conversion efficiency can reach 88%.

However, the experiment researches of RBS based on real vehicle has some disadvantages, such as high in cost, long in time, and large in resource-consuming. So one supercapacitor-based regenerative braking test bed is designed and some researches done based on the it.

## 2.Supercapacitor-based regenerative braking test bed design

The supercapacitor-based regenerative braking test bed is shown in figure 1. and it is mainly composed of three parts: the kinetic energy simulation module, the energy conversion and storage module, and the control module. The kinetic energy simulation module consists of a drive motor, a flywheel and two electromagnetic clutches, whose function is to simulate the inertia of the vehicle. The energy conversion and storage module comprises of a generator, a pulley drive, and a capacitor, which is used to convert the mechanical energy of the rotating flywheel into electrical energy and store it. The control module includes a main control unit, a human-computer interaction program, a speed sensor, a current sensor, and a voltage sensor, whose function is to monitor the rotational speed of the flywheel, current and voltage of the generator in real time, and control the power transmission between the kinetic energy simulation module and the energy conversion and storage module with the control of the electromagnetic clutch. The working process of the test bed is as follows: First, set the maximum speed of the flywheel, start the motor and engage the electromagnetic clutch A to connect the motor and the flywheel, the flywheel is driven by the motor. When the flywheel reaches the set maximum speed, the electromagnetic clutch A is disengaged and the driven process is completed.

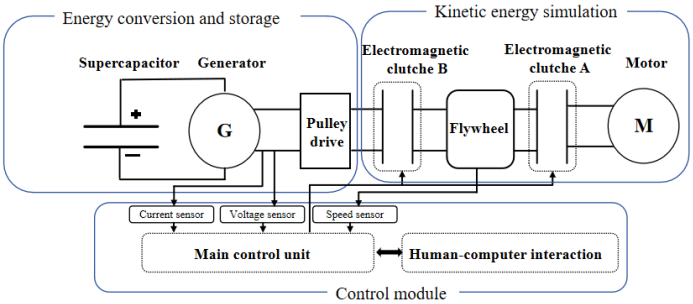


Fig.1 Diagram of the Regenerative braking test bed

Then the electromagnetic clutch B is engaged, and the kinetic energy of the flywheel is converted into electrical energy and is stored in the supercapacitor using the generator.

### 2.1 Flywheel design and selection

The kinetic energy of the vehicle is simulated by the rotating flywheel. From the safety perspective, the simulated object is a small beach vehicle, with a total weight of 150kg, a tire radius of 0.21m, and a maximum speed of 50km/h. The relationship between the flywheel and the vehicle speed is defined as formula (1):

$$\frac{1}{2}J_c\omega_1^2=\frac{1}{2}m_{car}v^2=\frac{1}{2}m_{car}(\omega_2 r)^2 \tag{1}$$

Where: $J_c$ is the moment of inertia of the flywheel, kg·m²; $\omega_1$ is the angular velocity of the flywheel, rad/s; $m_{car}$ is the mass of the simulated vehicle, kg; $v$ is the speed of the simulated vehicle, m/s; $\omega_2$ is the angular velocity of the simulated vehicle's wheels, rad/s; $r$ is the radius of the simulated vehicle's wheels, m.

Based on the simulated vehicle, the moment of inertia of the flywheel is 1.58kg·m². To meet the design requirements of the vehicle kinetic energy simulation system, two ZS195 single-cylinder diesel engine inertia flywheels are selected. The flywheel is cast with HT200 material, with a material density of 7000kg/m³, 425mm diameter and 100mm thickness. And it is moment of inertia is 1.6 kg·m².

### 2.2 Motor selection

In order to simulate the maximum speed of the vehicle (50km/h), the rotational speed of the flywheel should be faster than 1300r/min. To ensure the flywheel can smoothly accelerate from stationary to maximum speed within 30 seconds, the angular acceleration is calculated based on formula (2):

$$\frac{d\omega}{dt}=\frac{\Delta\omega}{\Delta t}=\frac{2\pi\times1300}{60\times30}=4.47rad/s^2 \tag{2}$$

Then the driving torque required by the flywheel transmission shaft is:

$$T = J_c \frac{d\omega}{dt} = 1.58 \times 4.47 = 7.06 N \cdot m \tag{3}$$

According to the design requirements of the drive system, a three-phase asynchronous motor is selected as the power source, with a rated speed parameter of 1440r/min. The motor is equipped with a frequency conversion speed control system, which can realize smooth start and precise speed control. The rated power of the motor is calculated based on formula (4):

$$P = \frac{T \times n}{9550} = \frac{7.14 \times 1440}{9550} = 1.06 kW \tag{4}$$

After system parameter matching and mechanical design manual verification, the YS-90L-6 three-phase asynchronous motor is finally determined. The key parameters of the motor include: 1.5kW rated output power, 380V working voltage, 9.8N·m rated torque characteristic. The motor is controlled by a frequency converter to realize start-up and speed adjustment.

### 2.3 Generator selection

According to the standard requirement, the braking distance of the vehicle should be less than 21m at an initial speed of 30km/h[13]. It is assumed that the braking process is a uniform deceleration motion, so the required braking torque is obtained from formula (5):

$$T_G = mar = \frac{mv^2 r}{2S} = 150 \times 1.64 \times 0.2 \approx 49.2 N \cdot m \tag{5}$$

Where: $S$ is the braking distance, m; $a$ is the braking deceleration, m/s². Then the relationship between the generator torque and power can be expressed by formula (6):

$$P = \frac{T_G n i}{9550} \tag{6}$$

Where: $i$ is the reduction ratio, and the value is 1/6 considering that the rotational speed of the DC generator is low.

The maximum power of the generator is 1.1kW based on the braking torque, maximum speed, and reduction ratio. Therefore, a 1.1kW generator is selected, and the detailed parameters of the generator are shown in Table 1.

*Table 1*

**Parameters of the generator**

| Model | Rated Voltage | Rated Power |
|---|---|---|
| JFZ2741B | 28V | 1.1kW |

### 2.4 Supercapacitor selection

The maximum voltage of the generator is 28V and the supercapacitor maximum voltage should be higher than the generator. So a 35V package supercapacitor with 100F capacity is assembled, which consists of 14

supercapacitors with rated voltage of 2.5V and capacity of 1400F in serial connection. Then the energy stored in the supercapacitor can be calculated by the following formula (7):

$$E = \frac{1}{2} \times C \times (U_{\max}^2 - U_{\min}^2) \tag{7}$$

Where: $E$ is the energy stored in supercapacitor, J; $C$ is the capacity of the supercapacitor, F; $U_{\max}$ is the maximum voltage of the supercapacitor, V; $U_{\min}$ is the minimum voltage of the supercapacitor, V.

The maximum stored energy of the supercapacitor is 61250J based on the calculation. The total kinetic energy released by the flywheel at the maximum rotational speed (1300r/min) is approximately 14648J, which is much less than the storage capacity of the supercapacitor. So the selected supercapacitor is capable of storing the total kinetic energy of the flywheel.

### 2.5 Selection of Electromagnetic Clutch

In the power transmission path of the test bed, the electromagnetic clutch not only achieves power coupling between the motor and the flywheel, but also regulates energy transmission between the flywheel and the generator. So, the torque transmission capacity should be higher than the driving torque of the driven shaft, which means the electromagnetic clutch should be greater than 7.06Nm, while the electromagnetic clutch B needs to be greater than 49.2Nm. And the key parameters of the electromagnetic clutch are shown in Table 2.

*Table 2*

**Parameters of of the electromagnetic clutch**

| | Model | Rated Power | Rated Torque | Maximum Rotational Speed |
|---|---|---|---|---|
| A | DED6-10A | 20V/1A | 10N.m | 2000r/min |
| B | DED6-40A | 20V/3A | 40N.m | 2000r/min |

### 2.6 Control system design

The control system includes a main controller, a data acquisition module, and a drive module. The main controller is a STM32F103VET6 single-chip controller, the rotational speed sensor is LQ-SDZ512, the voltage sensor is JK-D803, and the current sensor is JK-D800A.

This STM32F103VET6 single-chip controller is a 32-bit ARM architecture controller with a 72MHz main frequency computing capability, a dual-channel 12-bit precision analog-to-digital conversion module, 4 channels pulse signal processing functionality, and 4 groups of programmable digital output ports. So it is capable of sampling real-time voltage/current sensor data, realizing rotational speed monitoring, and controlling actuators such as electromagnetic clutches.

The voltage/current sensor can converted the input signals into a standard 0-3.3V signal via an internal conditioning circuit, which is connected to the ADC

channel of STM32 through an isolation circuit.

A dual-channel low-voltage driver chip IR4427 is selected to precisely control the operating state of the electromagnetic clutches. The circuit scheme is shown in Figure 2.

In addition, the motor of the test bed is only responsible for driving the flywheel, and its on and off state is achieved by manually.

The flow chart of the control system is shown in figure 3. First, the initialization is done to prepare for subsequent operations including the electromagnetic clutch A engagement and electromagnetic clutch B disengagement. Then, a desired rotational speed value will set and the rotational speed is monitoring. If the actual rotational speed is greater than the set rotational speed value, the system will perform the next operation; otherwise, it will continue to monitor the rotational speed. When the actual rotational speed is greater than the set value, the electromagnetic clutch A is disengaged while the electromagnetic clutch B is engaged. During program operation, the rotational speed of flywheel, current of generator, and voltage of generator are sampled in real time until the speed of flywheel reaches zero.

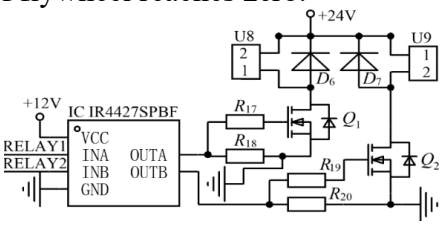


Fig.2 Scheme drive circuit of electromagnetic clutches

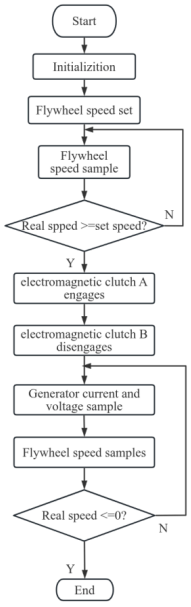


Fig.3 Flow chart of the control system

In order to control the experiment process, an MCGS configuration screen is used to design a human-computer interaction. This configuration screen has functions such as graphical interface design, logic control, and real-time curve components, and communicates with the STM32 microcontroller through the Modbus protocol.

The interface is shown in Figure 4. It consists speed set, sensor data show, model set. The speed set is used to set the desire speed of the flywheel. The model set is used to control the electromagnetic clutch, when the driven model is selected the electromagnetic clutch A is engaged and electromagnetic clutch B is disengaged while the recovery is selected the state of these two electromagnetic clutch reverses. The sensor data show is used to indicate the flywheel speed, generator current and voltage in real time.

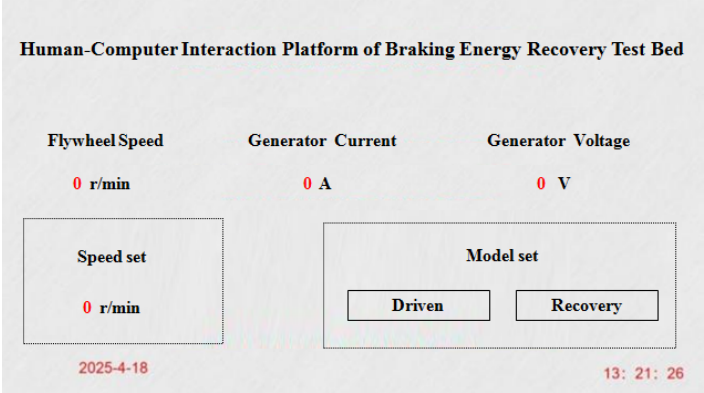


Fig.4 MCGS Configuration panel

## 3.Experiment test

After completing the design of the test bed and program debugging, the test bed is assembled and it is illustrated in Figure 5.

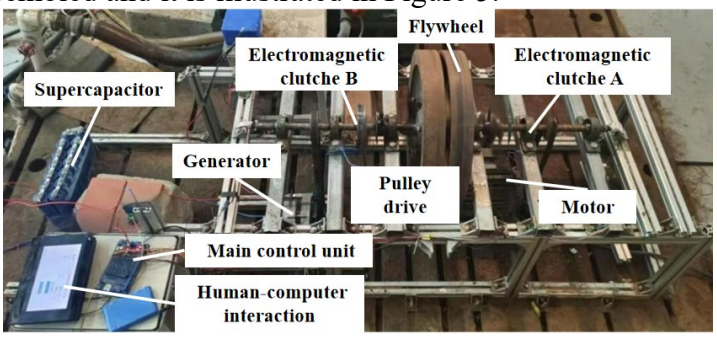


Fig.5 Real picture of the test bed

Firstly, the braking a braking energy recovery system are compared, as shown in Figure 6. It can be seen that the flywheel takes 280 seconds to stop

without the braking energy recovery system, while it only takes 39 seconds to stop when the generator is activated. It can be concluded that the braking energy recovery system can shorten the braking time compared with coasting. Then some test are done based on the test bed.

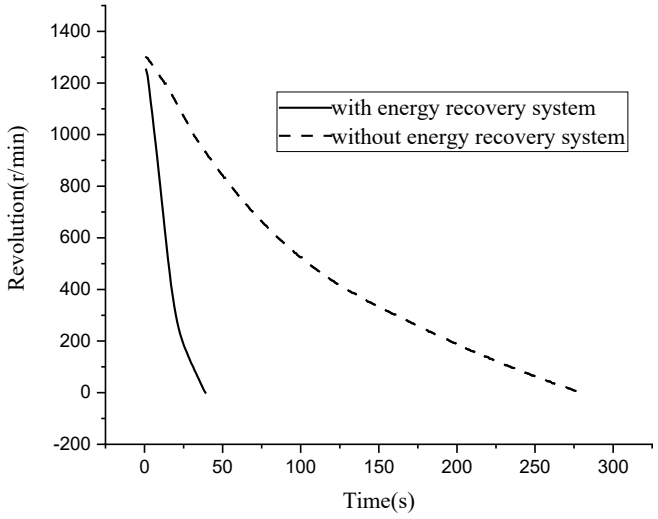


Fig.6 Braking processes with and without a braking energy recovery system

### 3.1 Influence of initial speed on energy recovery

As is known to all, the initial speed of the vehicle has a great influence on the braking process. Therefore, the influence of the initial speed on the braking energy recovery process is analyzed. The flywheel speed changes from 500r/min to 1300r/min, and the corresponding vehicle speed is from 19.44km/h to 50km/h.

#### 3.1.1 Influence of initial speed on braking distance

In order to show the influence of initial speed on braking distance, the braking distances is obtained by integrating the the curve of flywheel speed variation with time and it is shown in figure 7.

It can be seen from the figure that when the initial braking vehicle speed is 19.44km/h, the corresponding braking distance is 25.6m, when the speed is 50km/h, the braking distance increases to 155m. It is obvious that when the vehicle adopts the regenerative braking system, the initial vehicle speed is positively correlated with the braking distance.

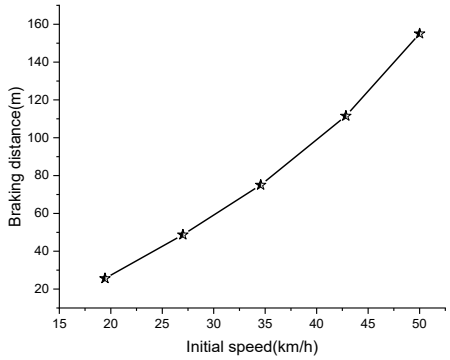


Fig.7 Braking Distances at different initial vehicle speeds

### 3.1.2 Influence of initial speed on regenerative energy efficiency

To better analyze the braking energy recovery changing with working conditions, the regenerative braking efficiency is introduced. This formula is derived from the law of conservation of energy, which can convert the regenerative braking efficiency corresponding to different vehicle speeds with formula (8).

$$\eta = \frac{\frac{1}{2} \times C \times (U_{\max}^2 - U_{\min}^2)}{\frac{1}{2} \times J_c \times \omega_1^2} = \frac{C \times (U_{\max}^2 - U_{\min}^2)}{J_c \times \omega_1^2} \tag{8}$$

Figure 8 shows the regenerative braking efficiency at different initial speeds. It can be seen from the figure that the regenerative braking efficiency is only 15.9% when the initial speed is 19.44km/h while the efficiency increases to 24.7% when the initial speed is 50km/h.

This efficiency improvement stems from energy conversion characteristics. When the flywheel is in high-speed working conditions, the kinetic energy stored in the flywheel is high and can drive generator to produce a stronger electromagnetic induction effect. The output voltage/current increase, accordingly, thereby enhancing the energy recovery effect. On the contrary, under low-speed operating conditions, the flywheel has insufficient kinetic energy. This prevents the generator from maintaining an effective electromagnetic field strength, which in turn leads to a reduction in electrical energy output and ultimately results in low energy recovery efficiency.

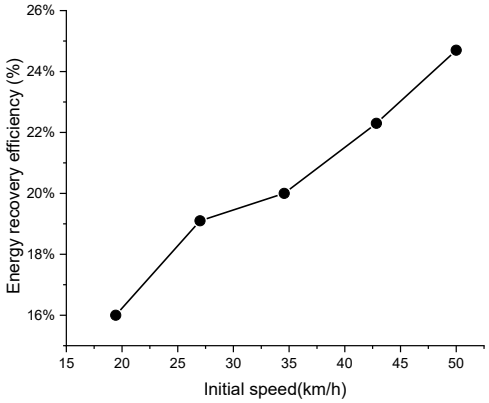


Fig.8 Regenerative braking efficiency at different speeds

### 3.2 Influence of transmission ratio on energy recovery

The pulley drive system comprises two pulleys, which determine the transmission ratio. Variations in the transmission ratio affect the generator's rotational speed, which in turn influences both the braking distance and power generation efficiency. For this reason, a comparative analysis was conducted between two scenarios: one with a transmission ratio of 1 and the other with a ratio of 1/6.

#### 3.2.1 Influence of transmission ratio on braking distance

The influence of the transmission ratio on the braking distance is shown in Figure 9. It can be seen from the figure that the braking distances corresponding to the three speed of 19.44km/h, 34.56km/h, and 50km/h are 69.5m, 212.5m, and 376.6m respectively when the transmission ratio is 1. And the braking distances are shortened to 26.5m, 75m, and 155m respectively when the transmission ratio is 1/6, with a decrease range of 61.9%-64.7%.

As the transmission ratio decreases, the rotational speed of the generator increases, with a consequent significant increase in the electromagnetic braking torque. A stronger damping braking effect is achieved through the enhanced Lenz current effect, thereby effectively shortening the braking stroke.

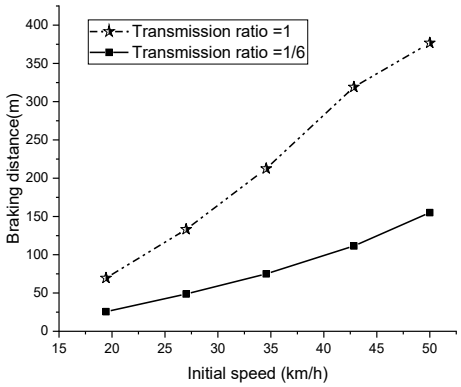


Fig.9 Braking distances at different transmission ratios

### 3.2.2 Influence transmission ratio on regenerative energy efficiency

The influence of the transmission ratio on energy recovery efficiency is shown in Figure 10. Experimental comparison shows that the regenerative energy efficiency raise to 21.48% from15.1% when the vehicle speed increase from 19.44 km/h to 50 km/h with a transmission ratio of 1. Meanwhile, the efficiency increased to 16%, 24.7%, which is 0.9% and 3.22% higher than that when the transmission ratio is 1/6 respectively.

The electromagnetic induction intensity and the generator revolution is quadratic proportional. Due to the transmission ratio decreases, the rotational speed of the generator increases significantly, and the resulting strong electromagnetic field makes the output voltage/current parameters optimized synchronously. Then the electromagnetic conversion efficiency of the regenerative braking system improve with the adjustment of the transmission ratio.

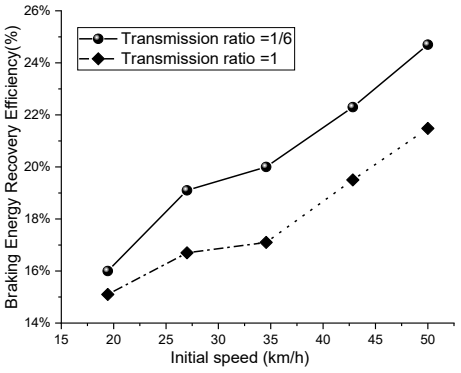


Fig.10 Braking energy recovery efficiency at different transmission ratio

The electromagnetic induction intensity is quadratically proportional to the

generator's rotational speed. As the transmission ratio decreases, the generator's rotational speed increases significantly. In turn, the strong electromagnetic field induced by this speed increase synchronously optimizes the generator's output voltage and current parameters. Consequently, the electromagnetic conversion efficiency of the regenerative braking system is enhanced with the adjustment of the transmission ratio.

### 3.3 Influence of Supercapacitor initial voltage on energy recovery

During the experiment, it is found that the initial voltage of the capacitor also has an impact on the energy recovery. So an analysis was conducted to study the relationship between the initial voltage of the capacitor and the energy recovery.

#### 3.3.1 Influence of initial voltage on braking distance

The influence of the capacitor's initial voltage on braking distance is illustrated in Figure 11. As shown in the figure, when the capacitor's initial voltage increases from 0 V to 10 V, the corresponding braking distance increases from 155 m to 168 m. It is evident that the braking distance becomes longer as the initial voltage rises.

This is because the braking distance is essentially determined by the deceleration rate of the flywheel, which in turn depends on the electromagnetic braking torque generated by the generator. A greater torque leads to a faster reduction in the flywheel's rotational speed, thereby resulting in a shorter braking distance. The relationship between generator current and torque can be defined as formula (9):

$$I = \frac{E_G - V}{R} = \frac{NBS\omega - V}{R} \tag{9}$$

Where: $I$ is the generator current, A; $E_G$ is the generator electromotive force, V ; $V$ is the voltage of the supercapacitor, V; $R$ is the total resistance of the circuit, Ω ; N is the number of coil turns;$B$ is the magnetic induction intensity, T; $S$ is the effective area of the coil, m²; ω is the angular velocity, rad/s.

Based on Formula (9), once the generator is selected, the initial electromotive force is determined by the initial rotational speed of the flywheel. When the initial voltage is 10 V, the $(E_G - V)$ value is smaller compared to when the initial voltage is 0 V. This smaller current results in a lower electromagnetic braking torque, which in turn leads to a longer braking distance.

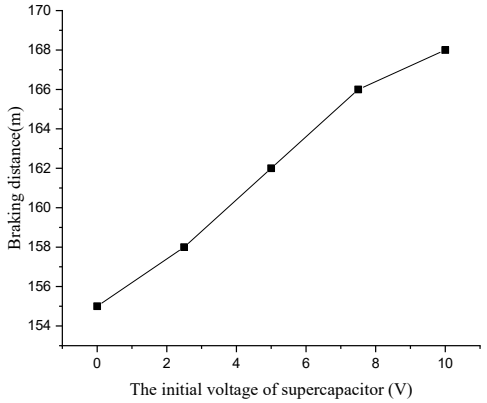


Fig.11 Braking distances at different supercapacitor initial voltage

### 3.3.2 Influence of initial voltage on regenerative energy efficiency

The effect of the initial voltage of the capacitor on energy recovery efficiency is shown in Figure 12. The experimental results show that when the initial voltage of the supercapacitor is 10V, its energy recovery efficiency is significantly higher than that when the initial voltage is 0V, and it can reach up to 53.2%, an increase of 28.5%.

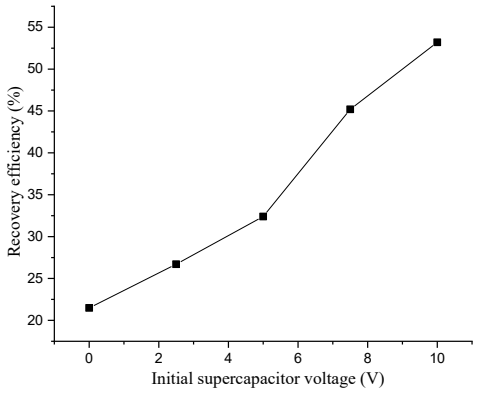


Fig.12 Recovery efficiency at different supercapacitor initial voltage

The regenerative energy efficiency is defined as the ratio of the energy absorbed by the supercapacitor to the initial kinetic energy of the flywheel. Therefore, when the initial kinetic energy is constant, the efficiency is determined by the amount of energy absorbed by the supercapacitor. The energy absorbed by the supercapacitor is affected by two key factors: energy loss during charging and the nonlinear characteristics of the supercapacitor's voltage variation. Compared with the scenario where the initial voltage is 10 V, during braking energy recovery

with an initial voltage of 0 V, the current is larger (as shown in Figure 13). This larger current leads to more significant Joule losses in the circuit resistance-much of the energy is dissipated as heat, reducing the actual energy stored in the supercapacitor.

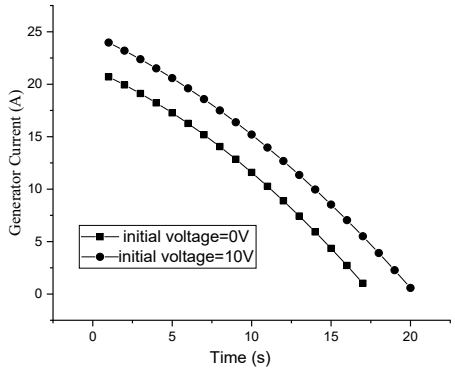


Fig.13 Current changes during energy recovery at different initial voltage

In addition, from the perspective of the relationship between charging efficiency and voltage range, when charging starts from 0 V, the supercapacitor's equivalent series resistance is relatively high in the low-voltage region, resulting in high energy loss in the early stage of charging. Moreover, the generator may operate in a nonlinear region due to an excessively low terminal voltage (near 0 V), leading to ineffective recovery of energy in the early phase of the process.

Thus, the energy recovery efficiency increases as the initial voltage of the supercapacitor rises.

## 4. Conclusions

In this paper, a supercapacitor-based regenerative braking test bed was developed to demonstrate the braking energy recovery process. Subsequently, a series of experiments were conducted using this test bed, and the key results are summarized as follows:

(1) Both the braking distance and regenerative energy efficiency increase with the initial speed. This is because the flywheel stores more kinetic energy under high-speed conditions, which enhances the electromagnetic induction effect of the generator-thereby promoting more effective energy conversion and improving recovery efficiency, while also leading to a longer braking distance due to the higher initial kinetic energy that needs to be dissipated.

(2) A lower transmission ratio significantly shortens the braking distance and improves regenerative energy efficiency. This can be attributed to the fact that a reduced transmission ratio increases the generator's rotational speed, which in

turn strengthens the electromagnetic braking torque and synchronously optimizes the generator's output voltage and current parameters, ultimately enhancing both braking performance and energy recovery effectiveness.

(3) A higher initial voltage of the supercapacitor extends the braking distance but improves energy recovery efficiency. When the initial voltage is low, the circuit experiences greater Joule losses; additionally, the generator may operate in a nonlinear region, and the supercapacitor exhibits high equivalent series resistance in the low-voltage range-these factors together result in ineffective energy recovery in the early stage. In contrast, a higher initial voltage avoids such issues, thereby boosting recovery efficiency, though it reduces the electromagnetic braking torque and lead to a longer braking distance.

In summary, the developed test bed achieves low-cost, controllable simulation of the regenerative braking process via MCU-based control, and provides a practical platform for understanding of regenerative braking systems.

**Acknowledgement**

This work was supported by scientific research and key project tackling initiative of Henan Province (Project No. 262102321088) . The authors would like to express their appreciation for the financial support from the Power-driven Machinery and Vehicle Engineering Research Center of Henan University of Engineering.

## REFERENCES

[1] *Kim D, Eo J S, Kim K. ,* "Parameterized energy-optimal regenerative braking strategy for connected and autonomous electrified vehicles: a real-time dynamic programming approach", in IEEE Access, **vol.** 9, no.1,Apr.2021, pp.103167-103183.

[2] *QIU Mingming, Yu Wei, Zhao Han, et al. ,* "Braking energy recovery control strategy for PHEVs considering coupling Influence of driving cycle and driving style", in China Mechanical Engineering,**vol.** 33, no.2, Jun.2022, pp.143-152.

[3] *WANG Rujie, WU Zhifei, Zou Chun. ,* "Study on Optimal Braking Energy Recovery Control Strategy of Pure Electric Logistics Vehicle", in Machinery Design & Manufacture, no.4, Jul.2022, pp.301-304.

[4] *ZHANG Junzhi, Lü Chen, LI Yutong, et al. ,* "Status quo and prospect of regenerative braking technology in electric cars", in Automotive Engineering, **vol.** 36, no.8, Feb.2014, pp. 911-918.

[5] *HE Ren, Zhu Siyu,* "Regenerative braking fuzzy control considering maximum braking energy recovery power", in Journal of Chongqing Institute of Technology, **vol.** 36, no.1, Apr. 2022, pp.1-11.

[6] *Zhang Yuanbo, Wang Weida, Zhang Hua, et al. ,* "Research on modified genetic algorithm-based high efficiency predictive regenerative braking control strategy for hybrid electric bus", in Journal of Mechanical Engineering, **vol.** 56, no.18, Apr.2020, pp. 105-115.

[7] *LI Hong, Chu Jiangwei, Sun Shufa, et al.,* "Characteristics of vehicle-mounted electromagnetic coupling flywheel energy storage system", in Energy Storage Science and Technology, **vol.** 10, no.5, Apr.2021,pp.1687-1693.
[8] *Ren Lu, Zhang Hongjuan, Jin Baoquan, et al. ,* "Study on charging and discharging characteristics of super capacitor in braking energy recovery system", in Electrical Measurement & Instrumentation, **vol.** 55, no.24, Dec.2018,pp.35-39+58.
[9] *Wu Jiayi, SU Zhijian, Yan Yangyi,* "Pneumatic braking energy recovery technology", in Chinese Hydraulics & Pneumatics, no.7, Sept. 2016,pp. 109-113.
[10] *Dong Han, Liu Xinhui, Wang Xin, et al. ,* "Parallel hydraulic hybrid braking regenerative characteristics", in Journal of Jilin University(Engineering and Technology Edition), **vol. 44**, no.6, Jun.2014, pp. 1655-1663.
[11] *Qu Jinyu, Wang Ru, Ren Chuanbo, et al. ,* "Analysis of testing and matching of braking energy recovery system of hydraulic energy storage type buses", in Chinese Hydraulics & Pneumatics, **vol.** 42, no.11, Dec.2014,pp. 9-11+15.
[12] *Fu Bisheng ,* Research and optimization of hydraulic regenerative braking energy recovery system based on dual accumulator. Zhejiang University of Technology, 2019.
[13] *Standardization Administration of the People's Republic of China.*Technical requirements and testing methods for commercial vehicle and trailer braking systems: GB12676-2014, Beijing: Standards Press of China, 2015.
[14] *Guo Zhihan, Kong Lingqian, LI Bin, et al. ,* "Design of fire extinguisher data acquisition experimental device based on single chip microcomputer", in Experimental Technology and Management, **vol.** 39, no.6, Jun.2022, pp.115-119.
[15] *Zhu Zhenyu, Wu Shuqun, Gu Yanan, et al. ,* "Development and teaching practice of image recognition system for high voltage discharge based on STM32", in Experimental Technology and Management, **vol.** 39, no.1, Feb.2022, pp.178-181.
[16] *Gao Xiquan, Ding Yumei.* ,Digital signal processing (fourth edition) , Xi'an:Xidian University Press, 2018.